Pramāṇa – J. Phys., Vol. 35, No. 6, December 1990, pp. 557–565. © Printed in India.

Form-factors for different aggregation models of micelles

P S GOYAL, K SRINIVASA RAO, B A DASANNACHARYA and V K KELKAR*

Solid State Physics Division, *Chemistry Division, Bhabha Atomic Research Centre, Bombay 400 085, India

MS received 10 May 1990; revised 23 July 1990

Abstract. Spherical micelles in ionic micellar solutions, often aggregate to form spherical, cylindrical or chain-like aggregates on addition of salt to the solution. It is known that the technique of small angle neutron scattering (SANS) can be used to distinguish spherical and cylindrical aggregates. To examine if SANS can be used to distinguish the latter two aggregation processes, we have calculated the angular distribution of scattered neutrons from 0·002 M CTAB solutions. These calculations show that aggregation of CTAB micelles results in large changes in SANS spectra. The shapes of SANS spectra are different for the above three types of aggregates, suggesting that technique of SANS can indeed be used to distinguish the three aggregation processes. The size of the aggregate can also be obtained from such studies.

Keywords. Micelles; form-factor; structure; small angle neutron scattering; cetyltrimethylammonium bromide.

PACS Nos 82·70; 61·20; 61·12

1. Introduction

Micellar solutions often show an increase in their viscosity on addition of a salt, solution of cetyltrimethylammonium bromide (CTAB) and sodium salicylate (NaSal) in water being an example (Rehege and Hoffman 1983; Shikata *et al* 1987). It is generally believed that increase in viscosity of micellar solution is connected with the fact that on addition of salt, two or more of CTAB micelles join to form bigger micelles or aggregates (Candau *et al* 1984; Shikata *et al* 1989; Goyal *et al* 1989). Several spherical CTAB micelles can, in general, join to form a larger spherical micelle, a cylindrical micelle or a chin (like a necklace) of spheres (Rao *et al* 1987; Brown *et al* 1989). In order to distinguish between these three aggregation processes, it is of interest to know if the angular distribution of the neutrons measured in small angle neutron scattering (SANS) experiment, would be different for the above three situations. In particular, it is of interest to know if SANS can be used to distinguish between a cylinder and a chain; this technique has been used to distinguish between a cylinder and a sphere (Kalus *et al* 1982). This paper reports calculated angular distribution of scattered neutrons for CTAB micellar solutions corresponding to above mentioned three aggregation processes and attempts to identify important regions of wave-vector transfer where the differences between these three types of structures manifest. The relevant expressions are given in the next section. Section 3 gives results of numerical calculations. The conclusions are summarized in §4.

2. Theory

Small angle neutron scattering (SANS) experiment measures the coherent differential scattering cross-section $d\Sigma/d\Omega$ as a function of the scattering vector $\bar{Q}$. The scattering vector $\bar{Q}$ is the difference vector between the wave vectors of the incident and scattered neutrons and has a magnitude $Q(=4\pi \sin \frac{1}{2}\phi/\lambda)$ where λ is the neutron wave length and ϕ is the scattering angle.

Expressions for $d\Sigma/d\Omega$ for several experimental situations have been discussed in the literature. In particular, expressions for $d\Sigma/d\Omega$ for dilute solutions of spherical and cylinderical micelles are known (Chen 1986). A similar expression for a micellar chain is given below. Before writing these expressions, it is useful to recall the approximations involved in deriving them. The general expression for coherent differential cross-section for scattering from a unit volume of solution is (Chen 1986; Hayter and Penfold 1983)

$$\frac{d\Sigma}{d\Omega}(\bar{Q}) = \left\langle \left| \sum_k b_k \exp(i\bar{Q}\cdot r_k) \right|^2 \right\rangle. \tag{1}$$

Here b_k is the neutron scattering length of kth atom located at r_k and the summation is over all the atoms in the unit volume of the solution. The angular brackets in (1) indicate an ensemble average.

The above expression can be simplified if one assumes that all micelles are identical (monodisperse). Let v be the volume of the micelle and n be the number of micelles in the unit volume of the solution. We further assume that the scattering length density ρ_m for the micelle is uniform over the volume of the micelle. This is reasonable as the distance scale at which one examines a sample in a SANS experiment is much larger than the inter atomic spacings. ρ_m is defined as

$$\rho_m = \frac{1}{v}\sum_v b_k, \tag{2}$$

where summation is over all the atoms in the micelle. The scattering length density ρ_s of the solution is given by an expression similar to (2). Within above approximations, eq. (1) can be simplified to

$$\frac{d\Sigma}{d\Omega}(Q) = n\langle |F(Q)|^2 \rangle + \left\langle \sum_{i=1}^{n}\sum_{j=1}^{n} F_i(Q)F_j^*(Q)\exp[i\bar{Q}\cdot(\bar{R}_i - \bar{R}_j] \right\rangle. \tag{3}$$

Here R_i is the co-ordinate of the centre of mass of the ith micelle and $F(Q)$ is the form factor of the micelle. $F(Q)$ is given by

$$F(Q) = \int_v d^3r(\rho_m - \rho_s)\exp(i\bar{Q}\cdot r), \tag{4}$$

where the integration is over the volume of the micelle. Thus we note that $d\Sigma/d\Omega$ (eq. 3) is made up of two terms; the first of which depends on intra-micelle scattering and the second on inter-micelle scattering. The intra-micelle term depends on the shape and size of the micelle and has been calculated for several shapes. It is, however, not straightforward to calculate the second term. The inter-micelle interference term depends not only on the spatial distribution of micelles but also on their relative

orientations. This can, however, be evaluated in a closed form for the case of spherical particles. In that case, eq. (3) can be simplified to (Hayter and Penfold 1983)

$$\frac{d\Sigma}{d\Omega}(Q) = n\langle|F(Q)|^2\rangle\left[1+\frac{1}{n}\sum_{i=1}^{n}\sum_{j=1}^{n}\exp\left[i\bar{Q}(\bar{R}_i-\bar{R}_j)\right]\right]$$
$$= n\langle|F(Q)|^2\rangle S(Q), \tag{5}$$

where $S(Q)$ is referred to as the structure factor. For nonspherical micelles, one has to use (3) instead of (5). At this stage, it may be mentioned that SANS has been widely used for studying shapes and sizes of micelles (Chen 1986). Most of these experiments have been performed on concentrated solutions and data have been analyzed in terms of (5). In this type of analysis, either one calculates $S(Q)$ assuming certain interaction potential between micelles (Chen 1986) or one examines the data in a limited Q region where $S(Q) \sim 1$ (Kalus *et al* 1982). To examine fine details of the shape of micelle, such as distinguishing between a chain and a cylinder, it is desirable that SANS experiments are performed on dilute solutions and that the data are put on absolute scale. Such results are at present not available.

For dilute solutions, inter-micelle interference effects are negligible ($S(Q) = 1$) and the second term in (3) can be ignored. That is, irrespective of the shape of the micelle, $d\Sigma/d\Omega$ for a dilute micellar solution is given by

$$\frac{d\Sigma}{d\Omega}(Q) = n\langle|F(Q)|^2\rangle. \tag{6}$$

It is common practice in literature to define the form factor $P(Q)$ for a micelle such that it is normalized to unity at $Q = 0$. That is, one rewrites (6) as

$$\frac{d\Sigma}{d\Omega}(Q) = n(\rho_m - \rho_s)^2 v^2 P(Q), \tag{7}$$

where

$$P(Q) = \frac{1}{v^2(\rho_m-\rho_s)^2}\langle|F(Q)|^2\rangle_Q. \tag{8}$$

Here $\langle\text{--}\rangle_Q$ denotes an average over all orientations of micelle relative to Q. This average over all directions is taken as the micelles are randomly oriented in the solution. The expressions for $P(Q)$ for different shapes of the micelle are given below:

(a) *Spherical micelle.* $P(Q)$ for a spherical micelle of radius R is given by (Rayleigh 1914)

$$P_{sp}(Q) = \left[\frac{3(\sin QR - QR\cos QR)}{(QR)^3}\right]^2. \tag{9}$$

(b) *Cylindrical (rod like) micelle.* The expression for $P(Q)$ for a cylindrical particle was derived by Guinier and Fournet (1955). They showed that if L_{cy} is length of cylinder and R is its radius, then

$$P_{cy}(Q) = \int_0^{\pi/2}\frac{4\sin^2(\frac{1}{2}Q\,L_{cy}\cos\beta)}{Q^2L_{cy}^2\cos^2\beta}\cdot\frac{4J_1^2(QR\sin\beta)}{Q^2R^2\sin^2\beta}\sin\beta\,d\beta, \tag{10}$$

where J_1 is the Bessel function of first order.

(c) *Micellar chain.* A micellar chain consists of a number of spherical micelles (beads) joined together. If $P_{sp}(Q)$ is the form factor of the spherical bead that constitutes the chain and K, the number of beads in the chain, it can be shown that form factor $P_{ch}(Q)$ of the chain is given by (Glatter 1980)

$$P_{ch}(Q) = P_{sp}(Q)\left[K + 2\sum_{i=1}^{K-1}\sum_{j=i+1}^{K}\frac{\sin(Qd_{ij})}{Qd_{ij}}\right] \tag{11}$$

where d_{ij} is the distance between the ith and the jth bead. Thus to calculate $P_{ch}(Q)$ for a chain, one needs the knowledge of shape of chain. In general, this chain is flexible and could have zigzag shape. If the chain is a Gaussian polymeric chain (possible for large K), one can use Debye's formulation (1947) to calculate the second term in (11). Here, we shall deal with short chains, which may be assumed to be straight and rigid. The distance d_{ij} between ith and jth bead in a straight chain is given by $d_{ij} = 2(i-j)R$ and $P_{ch}(Q)$ for such a chain reduces to

$$P_{ch}(Q) = P_{sp}(Q)\left[K + 2\sum_{i=1}^{K-1}\sum_{j=i+1}^{K}\frac{\sin\{2QR(i-j)\}}{\{2QR(i-j)\}}\right]. \tag{12}$$

3. Results of numerical calculations

We have calculated $d\Sigma/d\Omega$ for pure CTAB solution and for a solution containing small quantities of salt. The calculations have been done for CTAB concentration $C = 0{\cdot}002$ M in D_2O. In pure CTAB solutions, micelles are nearly spherical having radius $R \sim 25$ Å (Goyal *et al* 1989). For CTAB concentration of 0·002 M, there are about $n \sim 1{\cdot}2 \times 10^{16}$ micelles per ml of solution. At such a low concentration, the separation will be about 440 Å and intermicelle interference effects are expected to be entirely negligible. We, therefore, ignored interference effects and calculated $d\Sigma/d\Omega$ using (7) and (9). The results for pure CTAB solutions are shown in figure 1 by the lowest curve.

Coming to CTAB/D_2O/salt solutions, we recall that CTAB micelles aggregate in presence of salt. On addition of salt to the pure solution, let us assume that K CTAB micelles join to form spherical, cylindrical or a chain-like aggregate; the number density of these aggregates will be n/K. The aggregate will have a radius of $K^{1/3}R$ if it is spherical. For a cylindrical aggregate the length L_{cy} will be $4KR/3$ assuming a radius of R and if it is assumed to be a chain of original micelles, the length L_{ch} is $2KR$. Since the number density of the aggregates is smaller than that of CTAB micelles, it is expected that the interference effects in CTAB/D_2O/salt will be smaller than those in pure CTAB solutions. Cross-sections corresponding to the above three types of aggregates were, therefore, calculated using (9), (10) and (12) along with (7). The calculations have been done for $K = 3$, 6, 9 and 12. In case of a chain-like aggregate, we assume it to be a straight chain. This is not unreasonable for the above K values. The results are shown in figures 1 and 2.

Figure 1 shows $d\Sigma/d\Omega$ for CTAB/D_2O ($K = 1$) and CTAB/D_2O/salt solutions for $K = 6$. A comparison of distributions corresponding to $K = 1$ and $K = 6$, shows that aggregation of micelles results in large change in intensity of the scattered neutrons; the angular distribution of these neutrons depends on whether the aggregate is spherical, cylindrical or a micellar chain. The fact that SANS distributions are different for different shapes for $K = 6$, however, does not imply that SANS experiments can

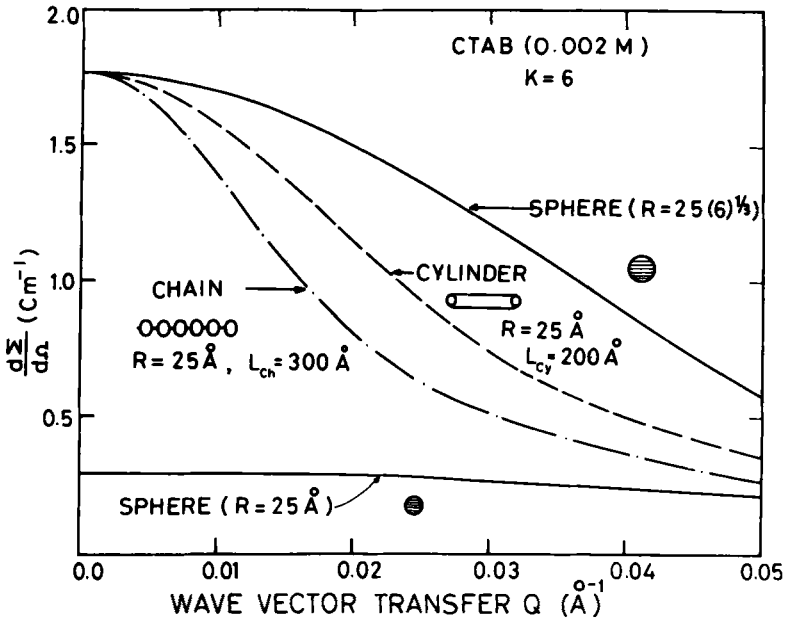

Figure 1. Calculated SANS spectra for 0·002 M CTAB/D_2O solution. The lower most curve corresponds to pure solutions where micelles are spherical (R = 25 Å). The upper three curves correspond to the solutions containing salt; it is assumed that on addition of salt, $K(=6)$ micelles join to form the aggregate. The different curves correspond to different geometries of the aggregates. The inter-aggregate interference effects have been neglected in these calculations.

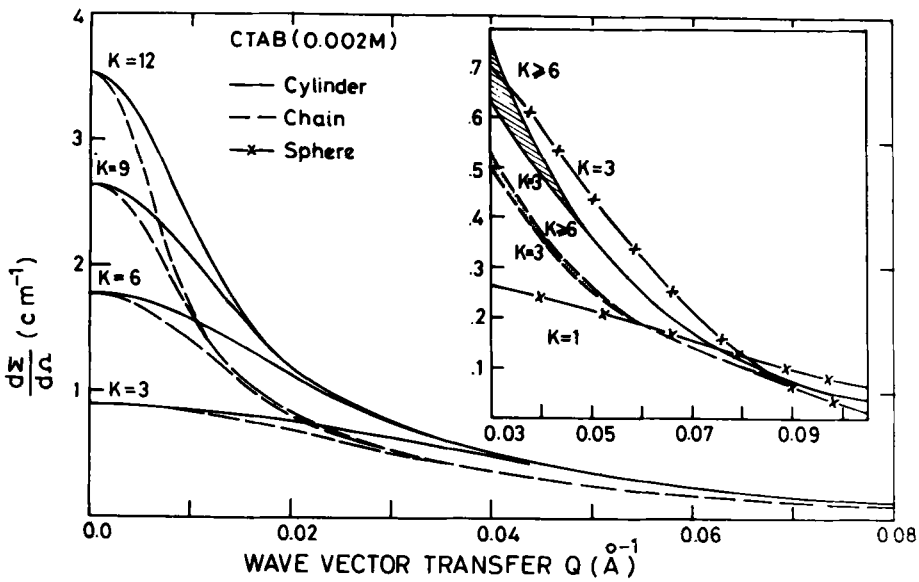

Figure 2. Calculated SANS spectra for 0·002 M CTAB/D_2O/salt solutions for different sizes (K) of the aggregates. The solid lines are for cylinders and the dashed for chains. Large Q data are shown in the inset The lower boundaries of the shadowed regions correspond to $K = 3$ and the upper boundries to $K > 6$. The inter aggregate interference effects have not been considered in these calculations.

be used to distinguish the above three shapes in a conclusive way. For example, it still remains to be clarified whether the angular distributions as observed for a given shape and K can be matched by another shape and a different K. To answer this question, we calculated and compared the SANS distribution for the three shapes for several values of K. The details of this comparison are given below in §§ 3a and 3b. Section 3c discusses calculation of $d\Sigma/d\Omega$ for somewhat concentrated solutions.

3a *Large Q Region*

The SANS distributions for cylinders (—), chains (---) and spheres (-- × --) for $K =$ 3, 6, 9 and 12 are shown in figure 2; the inset shows the distributions in region of larger Q in an expanded scale. It is seen that at large Q, $d\Sigma/d\Omega$ for a spherical aggregate is significantly different from that of an elongated aggregate (chain or cylinder). While SANS distribution for a spherical aggregate is very sensitive to K, it is almost independent of K for an elongated aggregate (see inset in figure 2). This is because of the fact that while the radius of the spherical aggregate increases with K, the radius of a cylindrical or a chain-like aggregate is independent of K. The increase in K, increases the length of an elongated aggregate and that effects only the low Q cross-sections. Thus a spherical aggregate can be easily distinguished from an elongated aggregate using large Q SANS data. On aggregation, the angular distribution of neutrons shows large changes at $Q \sim (K^{1/3}R)^{-1}$ for spherical aggregates; this does not happen for an elongated aggregate.

Coming to SANS from a chain and a cylinder, we note that for a given K, the calculated curve for a chain is always lower than that for a cylinder (figure 2). The increase in K, however, has a similar effect on the SANS distribution from a cylinder or a chain; larger the value of K, smaller is the value of Q where spectra corresponding to successive K values deviate from each other. The calculated distributions for cylinders and chains are independent of K at large $Q(> 0{\cdot}05\,\text{Å}^{-1})$. This is clearly seen in inset in figure 2; the upper boundries of the shadowed regions in the inset correspond to $K = 6$ and are valid for all values of K which are larger than six; the lower boundries correspond to $K = 3$. That is, it is seen that the SANS distributions from a chain and a cylinder are quite distinct though they have similar features. The shadowed region corresponding to the chain, for example, does not overlap with the shadowed region corresponding to the cylinder (inset in figure 2). This shows that large Q SANS data will definitely distinguish between a cylinder and a chain as long as $K > 3$. Thus, we conclude that for $K > 3$, it is possible to distinguish between spherical, cylindrical and chain-like aggregates using SANS data.

3b *Low Q region*

We note that in region of low $Q(< 0{\cdot}03\,\text{Å}^{-1})$, none of the dashed lines coincide with any of the solid lines (figure 2). That is, chains and cylinders of different lengths do not give similar cross-sections. To avoid confusion, the curves corresponding to spheres have not been plotted in low Q region. The SANS distribution from a spherical aggregate, for a given K, will be broader than that from a cylindrical aggregate. Thus, in principle, the size of the aggregate can be obtained using low Q SANS data. In short, we conclude that SANS experiments can not only be used to distinguish between the above three aggregation processes, but can also be used to obtain the size of the aggregate.

3c *Concentrated solutions*

In neutron experiments, scattered intensities are usually small. Thus, it is always desirable to use somewhat concentrated micellar solution rather than a very dilute one. Having established their usefulness for dilute solutions, we now examine if SANS experiments on somewhat concentrated solutions can be used to distinguish the various aggregation processes. For this, we have calculated the angular distribution of scattered neutrons for 0·008 M CTAB solution. The main difference between this calculation and the one reported above is, that calculation for 0·008 M solution takes account of inter-aggregate interference effects. The interference effects, however, have been calculated in an approximate way because of the reasons given below.

The calculation of interference effects is easy for spherical particles. For example, one can calculate $S(Q)$ using method of Hayter and Penfold (1981) and then use (5) for calculating the cross-section. The only parameters required for such a calculation of $d\Sigma/d\Omega$ are, the radius of the spherical aggregate and its charge. The calculation of inter-aggregate interference effects for elongated aggregates (chain or cylinder) are, however, quite involved. In general, the orientations of the elongated aggregates could be correlated, in which case (3) cannot be simplifed to (5). Even if the orientations of these aggregates were not correlated, it will not be possible to calculate $d\Sigma/d\Omega$ using (5) as the $S(Q)$ for elongated particles is not known. In view of above, we calculated the interference effects in an approximate way by assuming the aggregates to be spherical. Such an approximation has been used earlier also and it is believed that it will not change the final results drastically (Chen 1986). Thus we calculated $d\Sigma/d\Omega$ for 0·008 M CTAB solution using (5). The form factor $P(Q)$ of the aggregate was calculated using (9), (10) or (12) depending on the shape of the aggregate; $S(Q)$ was calculated using rescaled version of the method given by Hayter and Penfold (1981). The radius R used in calculating $S(Q)$ was of a sphere, which has the same volume as that of the aggregate; the charge on the aggregate was assumed to be Kq where $q(=26)$ is the charge on a single CTAB micelle in pure solution (Goyal *et al* 1989). The calculated distributions for $K = 6$ are shown in figure 3; the lowest curve is for pure CTAB solution and the upper three curves correspond to CTAB/salt solution. Again we note that SANS intensity from CTAB/salt solution is much larger than that for pure CTAB solution; This arises because of aggregation of CTAB micelles in presence of salt. The SANS distributions are different for different shapes of the aggregates, especially at large Q. Thus SANS experiments on somewhat concentrated solutions can also be used to obtain information about the shape of the aggregate. However, it will be difficult to obtain size information; the low Q cross-sections, which are senstive to the size of the aggregate, are considerably modified by $S(Q)$. SANS experiments on CTAB/NaSal and CTAB/KBr solutions for deciding the shapes of aggregates in these solutions are in progress.

4. Summary

Spherical micelles in ionic solutions, often aggregate to form spherical, cylindrical or chain-like aggregates on addition of salt. In this paper, we have investigated if the small angle neutron scattering experiments can be used to distinguish the above three aggregation processes. SANS distributions have been calculated for a dilute (0·002 M) and a somewhat concentrated (0·008 M) solution of CTAB. The calculations have

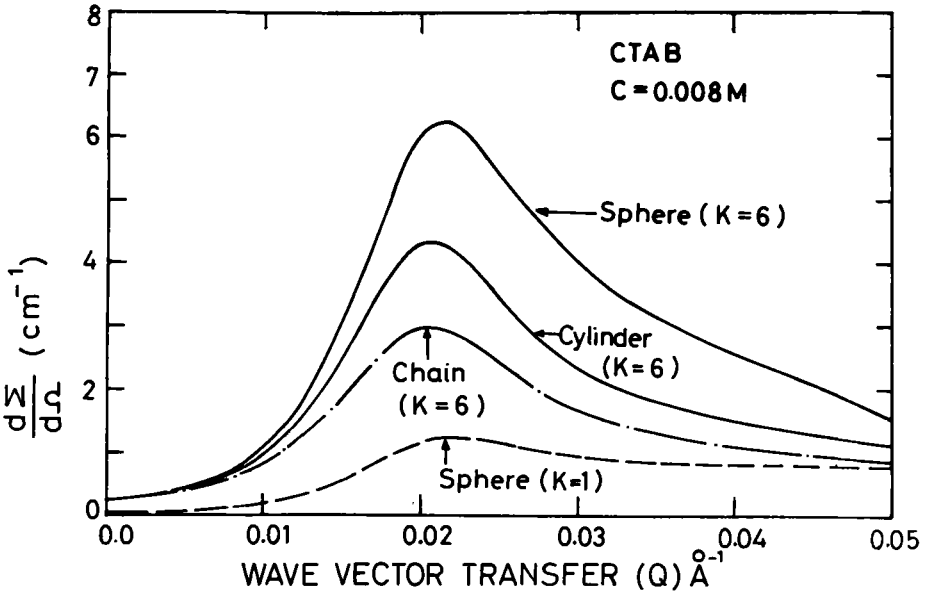

Figure 3. Calculated SANS spectra for 0·008 M CTAB solutions. The lowest curve corresponds to pure solution; the upper three curves correspond to solutions containing salt. It is assumed that on addition of salt $K(=6)$ micelles join to form the aggregate. In these calculations inter-aggregate interference effects have been incorporated in an approximate way (see text).

been done both for pure CTAB solutions and for solutions containing salt. It is assumed that on addition of salt, $K(=3, 6, 9$ and $12)$ spherical CTAB micelles ($R \sim 25$ Å) join to form the spherical, cylindrical or chain like-aggregate. The calculations on dilute solutions show that a SANS experiment can be used not only for distinguishing the three aggregation processes, but also for obtaining the size of the aggregate. It seems that experiments on concentrated solutions might also reveal the shape of the aggregates; but they cannot be used to obtain their sizes.

Acknowledgements

We thank Dr C Manohar and Shri S Basu for very useful discussions.

References

Brown W, Johansson K and Almgren M 1989 *J. Phys. Chem.* **93** 5888
Candau S J, Hirsch E and Zana R 1984 *J. Phys. (Paris)* **45** 1263
Chen S H 1986 *Annu. Rev. Phys. Chem.* **37** 351
Debye P 1947 *J. Phys. Colloid. Chem.* **51** 18
Glatter O 1980 *Acta Phys. Austriaca* **52** 243
Goyal P S, Chakravarthy R, Dasannacharya B A, Desa J A E, Kelkar V K, Manohar C, Narasimhan S L, Rao K R and Valaulikar B S 1989 *Physica* **156** 471
Guinier A and Fournet G 1955 *Small angle scattering of X-rays*, (New York: Wiley)

Hayter J B and Penfold J 1981 *J. Chem. Soc. Faraday Trans I* **77** 1851
Hayter J B and Penfold J 1983 *Colloid Polym. Sci.* **261** 1022
Kalus J, Hoffmann H, Reizlein K, Ulbricht and Ibel K 1982 *Ber. Bunsenges. Phys. Chem.* **86** 37
Rayleigh L 1914 *Proc. R. Soc. (London)* **A90** 219
Rao U R K, Manohar C, Valaulikar B S and Iyer R M 1987 *J. Phys. Chem.* **91** 3286
Rehege H and Hoffman H 1983 *Faraday Discuss. Chem. Soc.* **76** 363
Shikata T, Hirata H and Kotaka T 1987 *Langmuir* **3** 1081
Shikata T, Hirata H and Kotaka T 1989 *Langmuir* **5** 398